Accepted Manuscript

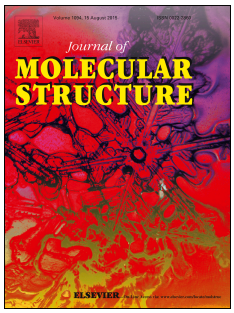

New 2-hydroxyethyl substituted N-Heterocyclic carbene precursors: Synthesis, characterization, crystal structure and inhibitory properties against carbonic anhydrase and xanthine oxidase

Aydın Aktaş, Samir Abbas Ali Noma, Duygu Barut Celepci, Fatoş Erdemir, Yetkin Gök, Burhan Ateş

PII: S0022-2860(19)30193-0

DOI: https://doi.org/10.1016/j.molstruc.2019.02.063

Reference: MOLSTR 26220

To appear in: *Journal of Molecular Structure*

Received Date: 8 December 2018

Revised Date: 1 February 2019

Accepted Date: 15 February 2019

Please cite this article as: Aydı. Aktaş, S.A. Ali Noma, D.B. Celepci, Fatoş. Erdemir, Y. Gök, B. Ateş, New 2-hydroxyethyl substituted N-Heterocyclic carbene precursors: Synthesis, characterization, crystal structure and inhibitory properties against carbonic anhydrase and xanthine oxidase, *Journal of Molecular Structure* (2019), doi: https://doi.org/10.1016/j.molstruc.2019.02.063.

New 2-Hydroxyethyl Substituted N-Heterocyclic Carbene Precursors: Synthesis, Characterization, Crystal Structure and Inhibitory Properties Against Carbonic Anhydrase and Xanthine Oxidase

Aydın Aktaş[a*], Samir Abbas Ali Noma[a], Duygu Barut Celepci[b], Fatoş Erdemir[a], Yetkin Gök[a], Burhan Ateş[a]

[1]*Department of Chemistry, Faculty of Arts and Sciences, Inönü University, 44280, Malatya, Turkey*
[2]*Dokuz Eylül University, Faculty of Sciences, Department of Physics, 35160-Buca, İzmir, Turkey*

*Corresponding Author: Aydın Aktaş

Address: Department of Chemistry

Inonu University, Malatya 44280, Turkey

Phone: 90-5356891975

Email: aydinaktash@hotmail.com

Abstract

Here, the synthesis, spectral and the structural studies of 2-hydroxyethyl substituted N-heterocyclic carbene (NHC) precursors and the enzyme inhibition activities of the NHC precursors were investigated against the cytosolic carbonic anhydrase I and II isoenzymes (hCA I and hCA II), and xanthine oxidase (XO). The IC_{50} values of NHC precursors against these enzymes were determined by spectrophotometric method. The spectra of new NHC precursors have been obtained by using ^{1}H NMR, ^{13}C NMR, FTIR spectroscopy and elemental analysis techniques. The structure of a new NHC precursor was established by using single-crystal X-ray diffraction method. The results of inhibition experiment indicated that all 2-hydroxyethyl substituted NHC derivatives showed remarkable inhibition activity toward hCA I, hCA II and XO. The range of IC_{50} values for hCA I, hCA II and XO inhibition was determined as 0.1565-0.5127, 0.1524-0.5368 and 1.253-5.342 µM. Especially, trimethylbenzyl derivative of 2-hydroxyethyl substituted NHC precursor has demonstrated high inhibition effect on all studied enzymes due to steric bulk of this substituent.

Keywords: Carbonic anhydrase; Crystal structure; Enzyme inhibition; *N*-heterocyclic carbene precursor; Xanthine oxidase.

1. Introduction

The first complex with the carbene ligand which is heteroatom and stabilized was prepared by Tschugajeff (English transcription, Chugaev) in 1925 [1]. The reactivity and stability of N-heterocyclic carbenes (NHC) were investigated by Wanzlick in the early 1960s [2]. Wanzlick and Öfele independently synthesized stable NHC transition metal complexes in 1968 [3]. Arduengo et al. discovered extraordinary stability, isolation, and storability of crystalline NHC IAd in 1991 [4]. Hence, NHC precursors have remained in the shadow of metal-NHC complexes for three decades. Numerous studies on NHCs were published after the stable NHC synthesis of Arduengo et al.

NHCs are neutral ligands that can be altered electronically and sterically. These ligands have strong σ-donor and weak π-acceptor properties [5-8]. In addition, NHC ligands that are resistant to the air and moisture can form stable complexes with most of the d-block and f-block metals. [9-14] Due to these unique properties, the NHC ligands are still alternative ligands to the phosphine ligands, which are often used in the industry [15].

NHC precursors and their metal complexes are of great interest in the fields of organic and organometallic synthesis. Numerous studies on the catalytic activity of the transition metal complexes of NHC ligands have been carried out for many years [16-22]. Several studies on the biological activities and medical applications of these complexes have been carried out in the last two decades [23-26]. Also, studies on the biological applications of NHC ligands have been carried out. From these studies, enzyme inhibition studies of NHC precursors are noteworthy [27-32].

Carbonic anhydrase (CA, carbonate hydrolase, E.C. 4.2.1.1) is a metalloenzyme that is very important for biological systems and contains a zinc (Zn^{+2}) ion in its active site [33-36]. CAs are important enzymes that have attracted considerable interest [37, 38]. CA inhibitors can serve as useful therapeutic agents for treating numerous diseases, including glaucoma, cancer, and obesity because of the roles of CAs in many physiological and pathophysiological processes, [39,40]. CA basically ensures that the CO_2 emerging from respiration is dissolved in water, transported and driven out of body as well as plays an important role in many physiological events such as acid-base balance, ion exchange, regulation of the cardiovascular system [41,42]. CA catalyzes the rapid and reversible hydration of carbon dioxide (CO_2) and water (H_2O) in

twostep reaction to yield bicarbonate (HCO_3^-) and a proton (H^+) to maintain acid-base balance in blood and other tissues, and to help transport CO_2 out of tissues in biological systems [43,44].

Xanthine oxidase (XO, EC 1.17.3.2) is a critical, rate-limiting enzyme in purine metabolism [45]. XO, a highly versatile flavoprotein enzyme, is ubiquitous among species (from bacteria to human) and within various tissues in mammals [46]. It catalyzes the last two steps of purine catabolism in humans, *i.e.*, hydroxylation of hypoxanthine to xanthine and xanthine to uric acid [47]. In parallel with the hydroxylation process, two kinds of reactive oxygen species (ROS), superoxide anion (O_2^-) and hydrogen peroxide (H_2O_2), are produced [48]. XO is therefore a critical source of uric acid and ROS. Over-production of uric acid can lead to hyperuricemia, which is the key cause of gout. XO is considered the most promising target for treating hyperuricemia and gout [49]. An increase in the excess of ROS production cause various pathological states including inflammation, metabolic disorders, atherosclerosis, cancer and chronic obstructive pulmonary disease [50, 51]. The inhibition of this enzyme would be beneficial to reduce the formation of ROS, knowing that its serum levels are significantly increased in various pathological states, like inflammation, ischemia-reperfusion, vascular diseases, and carcinogenesis [52]. Allopurinol is a prototypical XO inhibitor and has been widely used in the treatment of hyperuricemia and gout for several decades.

Previously, the synthesis of different 2-hydroxyethyl substituted metal-NHC complexes and their catalytic activities were investigated by our study group [53-55]. In this study, inhibition effects of a new series of 2-hydroxyethyl substituted NHC precursors on carbonic anhydrase and xanthine oxidase enzymes were investigated. The structure of a compound from the NHC precursors was established through the single-crystal X-ray diffraction method.

2. Experimental

All synthesis involving 2-hydroxyethyl substituted NHC precursors **1a-f** and **2a-c** were carried out under an inert atmosphere in flame-dried glassware using standard Schlenk techniques. The solvents were commercial products and were used without purification. All other reagents were purchased from Aldrich, Merck and Alfa Aesar Chemical Co, and used without further purification. Melting points were recorded in glass capillaries under air with an Electrothermal-9200 melting point apparatus. The UV-Vis absorption was obtained from a ethyl alcohol (C_2H_5OH) solution and recorded with a Shimadzu UV-1601 instrument UV-Vis

spectrophotometer. FTIR spectra were recorded in the range 400-4000 cm^{-1} on Perkin Elmer Spectrum 100 FT-IR spectrometer. ^{1}H and ^{13}C NMR spectra were recorded using a Bruker AS 400 Merkur spectrometer operating at 400 MHz (^{1}H) or 100 MHz (^{13}C) in $CDCl_3$ and DMSO-d_6 with tetramethylsilane as an internal reference. Elemental analyses were performed by İnönü University Scientific and Technological Research Center (Malatya, TURKEY).

Single-crystal X-ray diffraction data set of the complex **2a** was collected at room temperature on a Rigaku-Oxford Xcalibur diffractometer with an Eos-CCD detector using graphite-monochromated Mo-Kα radiation (λ = 0.71073 Å). Data collection and reduction along with absorption correction was performed using CrysAlis^{Pro} software package [56]. Structure solution was performed using *Intrinsic Phasing* method with SHELXT [57] package program embedded in the Olex2 [58]. Refinement of coordinates and anisotropic thermal parameters of non-hydrogen atoms were carried out by the full-matrix least-squares method in SHELXL [59]. All non-hydrogen atoms were refined anisotropically. Except the hydrogen of the hydroxyethyl oxygen atom, all hydrogen atom positions were calculated geometrically and refined using the riding model. The OH hydrogen was located in a difference Fourier map and refined freely. The details of the crystal data, data collection and structure refinement of the compound are summarized in Table 1.

Table 1. Crystal data and experimental details for the complex **2a.**

Empirical Formula	$C_{10}H_{13}IN_2O$
Formula Weight	304.12
Temperature (K)	293(2)
Crystal System, space group	Monoclinic, $P2_1/n$
a, *b*, *c* (Å)	9.3224(5), 8.8270(5), 14.4183(7)
β (^{0})	93.289(5)
V (Å^3)	1184.51(11)
Z	4
Density (calculated) (g/cm^3)	1.705
Absorbtion coefficient (μ, mm^{-1})	2.676
F(000)	592
Crystal size (mm^3)	0.416 × 0.354 × 0.290
Radiation	MoKα (λ=0.71073)

2θ range for data collection (^{0})	6.362 to 51.348
Index ranges	$-11 \leq h \leq 11$, $-5 \leq k \leq 10$, $-11 \leq l \leq 17$
Reflections collected	4287
Independent reflections	2256 [R_{int} = 0.019, R_{sigma} = 0.033]
Parameters	129
Goodness-of-fit on F^2	1.033
Final R indices [$I \geq 2\sigma(I)$]	R_1 = 0.033, wR_2 = 0.071
R indices	R_1 = 0.047, wR_2 = 0.078
Largest diff. peak/hole (eÅ^{-3})	0.45/-0.58

2.1. Synthesis of 1-(2-hydroxyethyl)-3-(2-methylbenzyl)benzimidazolium chloride, 1a

For the synthesis of **1a** as described in the literature [30], 2-methylbenzyl chloride (1.41 g, 10 mmol) and 1-(2-tetrahydro-pyran-2-yloxyethyl)benzimidazole (2.46 g, 10 mmol) was added in dry DMF (4 mL). Yield: 85 %; (2.57 g); m.p.: 147-149 °C; $\nu_{(CN)}$: 1557 cm^{-1}; $\nu_{(O-H)}$: 3175 cm^{-1}. Anal. Calc. for $C_{17}H_{19}ClN_2O$: C: 67.43; H: 6.32; N: 9.25. Found: C: 67.65; H: 6.40; N: 9.18. ^{1}H NMR (400 MHz, $CDCl_3$); δ 2.38 (s, 3H, -NCH$_2$(C$_6$H$_4$(C*H*$_3$)); 4.09 (s, 2H, -NC*H*$_2$CH$_2$OH); 4.78 (s, 2H, -NCH$_2$C*H*$_2$OH); 5.80 (s, 2H, -NC*H*$_2$(C$_6$H$_4$(CH$_3$)); 5.96 (s, 1H, -NCH$_2$CH$_2$O*H*); 7.16-7.84 (m, 4H, -N(C$_6$*H*$_4$)N- Ar-H); 10.68 (s, 1H, 2-C*H*). ^{13}C NMR (100 MHz, $CDCl_3$); δ 21.4 (-NCH$_2$(C$_6$H$_4$(*C*H$_3$)); 49.7 (-N*C*H$_2$CH$_2$OH); 51.6 (-N*C*H$_2$(C$_6$H$_4$(CH$_3$)); 59.0 (-NCH$_2$*C*H$_2$OH); 113.6, 113.8, 126.9, 127.0, 128.7, 128.8, 129.2, 130.0, 131.2, 131.4, 131.9, 132.5, 132.7 and 139.3 (Ar-C); 143.4 and 143.9 (2-*C*H).

2.2. Synthesis of 1-(2-hydroxyethyl)-3-(3-methylbenzyl)benzimidazolium chloride, 1b

The synthesis of **1b** was carried out in the same method as that described for **1a**, but 3-methylbenzyl chloride (1.41 g, 10 mmol) was used instead of 2-methylbenzyl chloride. Yield: 91 % (2.75 g); m.p.: 110-112 °C; $\nu_{(CN)}$: 1559 cm^{-1}; $\nu_{(O-H)}$: 3237 cm^{-1}. Anal. Calc. for $C_{17}H_{19}ClN_2O$: C: 67.43; H: 6.32; N: 9.25. Found: C: 67.58; H: 6.41; N: 9.21. ^{1}H NMR (400 MHz, $CDCl_3$); δ 2.24 (s, 3H, -NCH$_2$(C$_6$H$_4$(C*H*$_3$)); 4.08 (s, 2H, -NC*H*$_2$CH$_2$OH); 4.70 (s, 2H, -NCH$_2$C*H*$_2$OH); 5.64 (s, 2H, -NC*H*$_2$(C$_6$H$_4$(CH$_3$)); 5.77 (s, 1H, -NCH$_2$CH$_2$O*H*); 7.04-7.77 (m, 4H, -N(C$_6$*H*$_4$)N- Ar-H); 10.76 (s, 1H, 2-C*H*). ^{13}C NMR (100 MHz, $CDCl_3$); δ 21.2 (-NCH$_2$(C$_6$H$_4$(*C*H$_3$)); 49.6 (-

N*C*$H_2$$CH_2$OH); 51.5 (-N*C*$H_2$($C_6H_4$($CH_3$)); 58.7 (-$NCH_2$*C*$H_2$OH); 113.0, 113.7, 113.8, 127.0, 128.2, 128.3, 129.5, 129.7, 130.1, 131.2, 131.9 and 139.3 (Ar-C); 143.4 (2-*C*H).

2.3. Synthesis of 1-(2-hydroxyethyl)-3-(4-methylbenzyl)benzimidazolium chloride, 1c

The synthesis of **1c** was carried out in the same method as that described for **1a**, but 4-methylbenzyl chloride (1.41 g, 10 mmol) was used instead of 2-methylbenzyl chloride. Yield: 88 % (2.66 g); m.p.: 135-137 °C; $\nu_{(CN)}$: 1562 cm^{-1}; $\nu_{(O-H)}$: 3305 cm^{-1}. Anal. Calc. for $C_{17}H_{19}ClN_2O$: C: 67.43; H: 6.32; N: 9.25. Found: C: 67.59; H: 6.42; N: 9.19. ^{1}H NMR (400 MHz, $CDCl_3$); δ 2.24 (s, 3H, -NCH_2(C_6H_4(C*H*$_3$)); 4.08 (s, 2H, -NC*H*$_2$$CH_2$OH); 4.70 (s, 2H, -$NCH_2$C*H*$_2$OH); 5.64 (s, 2H, -NC*H*$_2$($C_6H_4$($CH_3$)); 5.77 (s, 1H, -$NCH_2CH_2$O*H*); 7.09-7.68 (m, 4H, -N(C_6*H*$_4$)N- Ar-H); 10.89 (s, 1H, 2-C*H*). ^{13}C NMR (100 MHz, $CDCl_3$); δ 21.2 (-NCH_2(C_6H_4(*C*H_3)); 49.6 (-N*C*$H_2$$CH_2$OH); 51.5 (-N*C*$H_2$($C_6H_4$($CH_3$)); 58.7 (-$NCH_2$*C*$H_2$OH); 113.0, 113.7, 127.0, 128.2, 128.3, 129.4, 130.1, 131.2, 131.9, 132.6 and 139.3 (Ar-C); 143.4 (2-*C*H).

2.4. Synthesis of 1-(2-hydroxyethyl)-3-(2,4,6-trimethylbenzyl)benzimidazolium chloride, 1d

The synthesis of **1d** was carried out in the same method as that described for **1a**, but 2,4,6-trimethylbenzyl chloride (1.69 g, 10 mmol) was used instead of 2-methylbenzyl chloride. Yield: 83 % (2.74 g); m.p.: 181-183 °C; $\nu_{(CN)}$: 1557 cm^{-1}; $\nu_{(O-H)}$: 3241 cm^{-1}. Anal. Calc. for $C_{19}H_{23}ClN_2O$: C: 68.97; H: 7.01; N: 8.47. Found: C: 69.09; H: 7.11; N: 8.51. ^{1}H NMR (400 MHz, $CDCl_3$); δ 2.20-2.23 (s, 9H, -NCH_2(C_6H_2(C*H*$_3$)$_3$); 3.94 (s, 2H, -NC*H*$_2$$CH_2$OH); 4.67 (s, 2H, -$NCH_2$C*H*$_2$OH); 5.63 (s, 2H, –NC*H*$_2$($C_6H_2$($CH_3$)$_3$); 5.78 (s, 1H, -$NCH_2CH_2$O*H*); 6.86 (s, 2H, –$NCH_2$($C_6$*H*$_2$($CH_3$)$_3$); 7.38-7.86 (m, 6H, Ar-H); 9.93 (s, 1H, 2-C*H*). ^{13}C NMR (100 MHz, $CDCl_3$); δ 20.1-21.1 (-NCH_2(C_6H_2(*C*H_3)$_3$); 46.7 (-N*C*$H_2$$CH_2$OH); 49.9 (-N*C*$H_2$($C_6H_2$($CH_3$)$_3$); 59.1 (-$NCH_2$*C*$H_2$OH); 113.4, 113.6, 124.8, 126.2, 126.3, 127.1, 128.8, 129.2, 130.1, 131.1, 131.4, 131.9, 138.0, 138.1 and 139.8 (Ar-**C**); 142.3 (2-*C*H).

2.5. Synthesis1-ethyl-3-(2-hydroxyethyl)benzimidazolium bromide, 1e

The synthesis of **1e** was carried out in the same method as that described for **1a**, but ethyl bromide (1.1 g, 10 mmol) was used instead of 2-methylbenzyl chloride. Yield: 88 % (2.38 g); m.p.: 96-98 °C $\nu_{(CN)}$: 1560 cm^{-1}; $\nu_{(O-H)}$: 3325 cm^{-1}. Anal. Calc. for $C_{11}H_{15}BrN_2O$: C: 48.72; H:

5.58; N: 10.33. Found: C: 48.79; H: 5.62; N: 10.31. ^{1}H NMR (400 MHz, $CDCl_3$); δ 1.65 (t, 3H, *J* = 8 Hz -NCH_2CH_3); 3.90 (s, 1H, -NCH_2CH_2OH); 4.02 (t, 2H, *J* = 6 Hz -NCH_2CH_2OH); 4.54 (t, 2H, *J* = 6.7 Hz -NCH_2CH_3); 4.72 (t, 2H, *J* = 4 Hz -NCH_2CH_2OH); 7.52-7.85 (m, 4H, -$N(C_6H_4)$N- Ar-*H*); 10.42 (s, 1H, 2-C*H*). ^{13}C NMR (100 MHz, $CDCl_3$); δ 14.7 (–NCH_2CH_3); 43.0 (-NCH_2CH_2OH); 59.5 (-NCH_2CH_2OH); 49.8 (-NCH_2CH_3); 113.0, 114.0, 127.0, 127.1, 127.8, 131.0, 131.2 and 131.9. (Ar-*C*); 141.7 (2-*C*H).

2.6. Synthesis of 1-(2-hydroxyethyl)-3-isopropylbenzimidazolium bromide, 1f

The synthesis of **1f** was carried out in the same method as that described for **1a**, but isopropyl bromide (1.23 g, 10mmol) was used instead of 2-methylbenzyl chloride. Yield: 79 % (2.25 g); m.p.: 146-147 °C; $\nu_{(CN)}$: 1548 cm^{-1}; $\nu_{(O-H)}$: 3323 cm^{-1}. Anal. Calc. for $C_{12}H_{17}BrN_2O$: C: 50.54; H: 6.01; N: 9.82. Found: C: 50.61; H: 6.06; N: 9.79. ^{1}H NMR (400 MHz, $CDCl_3$); δ 1.78 (d, 6H, *J* = 4 Hz -$NCH(CH_3)_2$); 4.08 (s, 2H, -NCH_2CH_2OH); 4.10 (s, 1H, -NCH_2CH_2OH); 4.80 (s, 2H, -NCH_2CH_2OH); 4.92 (m, 1H,-$NCH((CH_3)_2)$; 7.57-7.81 (m, 4H, -$N(C_6H_4)$N- Ar-*H*); 10.36 (s, 1H, 2-C*H*). ^{13}C NMR (100 MHz, $CDCl_3$); δ 22.4 (–$NCH(CH_3)_2$); 49.6 (-NCH_2CH_2OH); 51.9 (–$NCH(CH_3)_2$); 59.1 (-NCH_2CH_2OH); 113.4, 113.8, 127.1, 127.3, 130.6 and 132.1. (Ar-***C***); 140.4 (2-***C***H).

2.7. Synthesis of 1-(2-hydroxyethyl)-3-methylbenzimidazolium iodide, 2a

For the synthesis of **2a** as described in the literature [30], 1-methylbenzimidazole (1.3 gr, 10 mmol) and 2-iodoethanol (1.25 g, 10 mmol) was added in DMF (4 mL). Yield: 83 % (2 g); m.p.: 148-150 ^{0}C, $\nu_{(CN)}$: 1568 cm^{-1}; $\nu_{(O-H)}$: 3326 cm^{-1}. Anal. Calc. for $C_{10}H_{13}IN_2O$: C: 39.49; H: 4.31; N: 9.21. Found: C: 39.41; H: 4.27; N: 9.15. ^{1}H NMR (400 MHz, DMSO-d_6), δ 4.12 (s, 3H, NCH_3); 4.57 (t, 2H, J: 4, NCH_2CH_2OH); 3.83 (m, 2H, *J:* 6.6, NCH_2CH_2OH); 5.19 (s, 1H, NCH_2CH_2OH); 7.72-8.10 (m, 4H, Ar-***H***); 9.69 (2-C***H***). ^{13}C NMR (100 MHz, DMSO-d_6), δ 33.7 (NCH_3); 49.9 and 5.1 (NCH_2CH_2OH); 114.0, 114.2, 126.8, 126.9, 131.6 and 132.3 (Ar-***C***); 143.4 (2-***C***H).

2.8. Synthesis of 1-ethyl-3-(2-hydroxyethyl)benzimidazolium iodide, 2b

The synthesis of **2b** was carried out in the same method as that described for **2a**, but 1-ethylbenzimidazole (1.5 g, 0.6 mmol) was used instead of 1-methylbenzimidazole. Yield: 80 % (2.25 g); m.p.: 135-136 °C; $\nu_{(CN)}$: 1566 cm^{-1}; $\nu_{(O-H)}$: 3341 cm^{-1}. Anal. Calc. for $C_{11}H_{15}IN_2O$: C: 41.53; H: 4.75; N: 8.81. Found: C: 41.49; H: 4.70; N: 8.76. ^{1}H NMR (400 MHz, DMSO-d_6), δ 1.53 (t, 3H, *J*=7,3 Hz, -$NCH_2C\boldsymbol{H}_3$); 5.37 (s, 1H, -$NCH_2CH_2O\boldsymbol{H}$); 4.50 (m, 2H, -$NCH_2C\boldsymbol{H}_2OH$); 4.53 (t, 2H, *J*=5.0 Hz, $NC\boldsymbol{H}_2CH_2OH$); 2.51 (m, 2H, J:1.6, $NC\boldsymbol{H}_2CH_3$); 7.66-8.03 (m, 4H, Ar-***H***); 9.59 (2-C***H***). ^{13}C NMR (100 MHz, DMSO-d_6), δ 14.6 ($NCH_2\boldsymbol{C}H_3$); 42.6 and 49.9 ($N\boldsymbol{C}H_2\boldsymbol{C}H_2OH$); 59.1 ($N\boldsymbol{C}H_2CH_3$); 113.9, 114.2,127.1, 131.3 and 131.7 (Ar-***C***); 142.1 (2-***C***H).

2.9. Synthesis of 1-(2-hydroxyethyl)-3-isopropylbenzimidazolium iodide, 2c

The synthesis of **2c** was carried out in the same method as that described for **2a**, but 1-isopropylbenzimidazole (1.5 g, 0.6 mmol) was used instead of 1-methylbenzimidazole. Yield: 70 % (2.1 g); m.p.: 135-137 ^{0}C, $\nu_{(CN)}$: 1557 cm^{-1}. $\nu_{(O-H)}$: 3306 cm^{-1}. Anal. Calc. for $C_{12}H_{17}IN_2O$: C: 43.39; H: 5.16; N: 8.43. Found: C: 43.35; H: 5.13; N: 8.39. ^{1}H NMR (400 MHz, $CDCl_3$), δ 1.77 (d, 6H, *J*=6.7 Hz, $NCH(C\boldsymbol{H}_3)_2$); 4.63 (s, 1H, $NCH_2CH_2O\boldsymbol{H}$); 4.09 (t, 2H, *J*=4.8 Hz, $NCH_2C\boldsymbol{H}_2OH$); 4.79 (t, 2H, *J*=4.0 Hz, $NC\boldsymbol{H}_2CH_2OH$); 4.92 (m, 1H, J:6.6 Hz, $NC\boldsymbol{H}(CH_3)_2$); 7.57-7.82 (m, 4H, Ar-***H***); 10.32 (2-C***H***). ^{13}C NMR (100 MHz, $CDCl_3$), δ 22.4 ($NCH(\boldsymbol{C}H_3)_2$); 49.6 and 51.9 ($N\boldsymbol{C}H_2\boldsymbol{C}H_2OH$); 59.1 ($N\boldsymbol{C}H_2(CH_3)_2$); 113.4, 113.8, 127.1, 127.3, 130.6 and 132.1 (Ar-***C***); 140.4 (2-***C***H).

2.10. Purification of hCA isoenzymes and esterase activity assay

The purification and inhibition studies hCA I and II isoenzymes were purified according to methods described by Gocer et al [60]. The protein quantity in the purification step was also determined spectrophotometrically at 280 nm. For visualizing of both CA isoenzymes purity, sodium dodecyl sulphate-polyacrylamide gel electrophoresis (SDS-PAGE) was performed. The esterase activity of CA isoenzymes was measured according to the method described by Verpoorte et al [61]. The change in absorbance at 348 nm of 4-nitrophenylacetate (NPA) to 4-nitrophenylate was recorded spectrophotometrically for 3 min at room temperature. NPA was used as the substrate (Figure 1). The reaction mix contained 50 mM Tris–SO_4 buffer (pH 7.4), 3.0 mM 4-NPA, distilled water, and purified enzyme. The inhibition studies of the esterase's were carried out by adding of inhibitor substance at different concentrations to the medium instead of

part of the distilled water. Inhibitory activity was expressed as IC50 values (the concentration at which 50 % of the enzyme activity inhibited), which were calculated using Graphpad Prism 5.0 from a dose-response curve. Each experiment was carried out as triplicates.

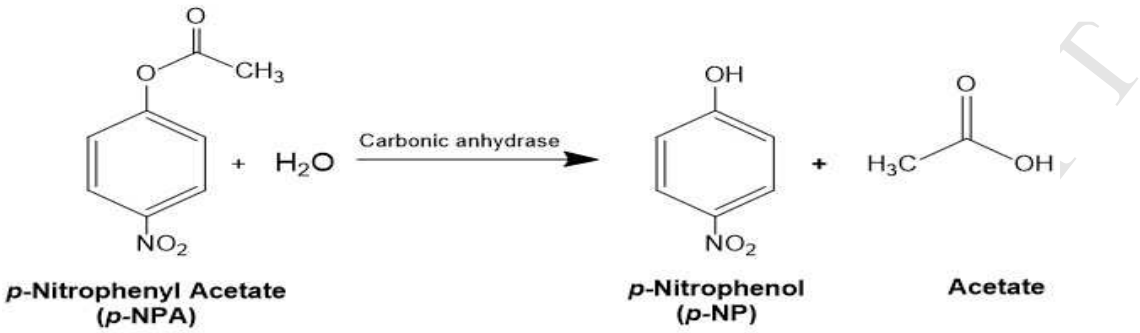

Figure 1. The mechanism in the conversion of 4-nitrophenylacetate to 4-nitrophenol by Carbonic anhydrases.

2.11. Xanthine oxidase activity assay

XO activity was determined by quantifying the amount of uric acid produced from xanthine in the reaction mixture. Inhibition of XO catalyzed reaction was measured by observing the decrease in the uric acid formation at 294 nm. The reaction mixtures contain 0.2 U XO, 50 mM phosphate buffer (pH 7.4), different concentration of tested compounds and 1 mM xanthine prepared freshly was added to initiate the reaction. The reaction mixture was incubated for 10 min at 37 °C before added xanthine, then xanthine was added to start the reaction and the activity was measured at wavelength 294 nm. All the experiments were performed in triplicates, then the average of three reading was taken. Allopurinol was used as a positive control. Then inhibition percentage (IC_{50}) of XO was founded in terms to decrease in uric acid formation as compared to the product formation in absence of inhibitor. Supporting information includes sample graph that enzyme inhibition activities are monitored by the absorption pattern as function of time for XO. The percent inhibition (IC_{50}) of XO activity was calculated as the following:

Xanthine oxidase inhibition (%) = $(A_{control} - A_{sample} / A_{control})100$

3. Results and discussion

3.1. Synthesis of 2-hydroxyethyl substituted NHC Precursors (1a-f and 2a-c)

The 2-hydroxyethyl substituted NHC precursors were synthesized successfully that have been illustrated in Scheme 1 and Scheme 2. The compounds **1a–f** have been synthesized from the 1-(2-tetrahydro-pyran-2-yloxyethyl)benzimidazole and alkyl/aryl halide (2-methylbenzyl chloride, 3-methylbenzyl chloride, 4-methylbenzyl chloride, 2,4,6-trimethylbenzyl chloride, ethyl bromide, isopropyl bromide). The compounds **2a–c** have been synthesized from the *N*-alkylbenzimidazole (Alkyl: methyl, ethyl and isopropyl) and 2-iodoethanol. The chemical structures of all compounds were confirmed by ^{1}H NMR, ^{13}C NMR, FTIR spectroscopy and elemental analysis techniques. The air and moisture stable NHC precursors are soluble both in polar solvents such as water, dimethylsulfoxide and in halogenated solvents such as dichloromethane and chloroform. The NHC precursors (chlorinated and brominated salts) **1a-f** were obtained as a white solid in between 79 % and 91 % yield. The NHC precursors (iodized salts) **2a-c** were obtained as a yellow-brown solid in between 70 % and 83 % yield. The formation of the 2-hydroxyethyl substituted NHC precursors **1a–f** and **2a–c** was confirmed by FT-IR, ^{1}H NMR and ^{13}C NMR spectroscopic methods and elemental analysis techniques. These spectra are consistent with the proposed formulate. In the ^{1}H NMR spectra, the 2-hydroxyethyl substituted NHC precursors were identified by a characteristic proton peak at the 2-position (NC***H***N) of the NHC precursors, which appeared highly downfield shifted singleds at δ 10.68, 10.76, 10.81, 9.93, 10.42, 10.36, 9.69, 9.59 and 10.32 ppm for **1a-f** and **2a-c**, respectively. The N***C***HN carbon resonances of these NHC precursors in the ^{13}C NMR spectra appeared highly downfield shifted at δ 143.9, 143.4, 143.4, 142.3, 141.7, 140.4 143.4, 142.1 and 140.4 ppm for (**1a-f** and **2a-c)**, respectively. The results of the elemental analysis were evaluated and it was observed that the calculated values were very close to the found values. The FTIR data clearly indicated the presence of $\nu_{(CN)}$ 1557, 1559, 1562, 1557, 1560, 1548, 1568, 1566 and 1557 cm^{-1} for the NHC precursors **1a–f** and **2a-c,** respectively. The FTIR data clearly indicated the presence of $\nu_{(OH)}$ 3175, 3237, 3305, 3241, 3325, 3323, 3326, 3341 and 3306 cm^{-1} for the NHC precursors **1a–f** and **2a-c,** respectively. All spectroscopic data are consistent with the literature [29-31]. In this study, we obtained a single crystal for NHC precursor **2a** by using the X-ray diffraction method.

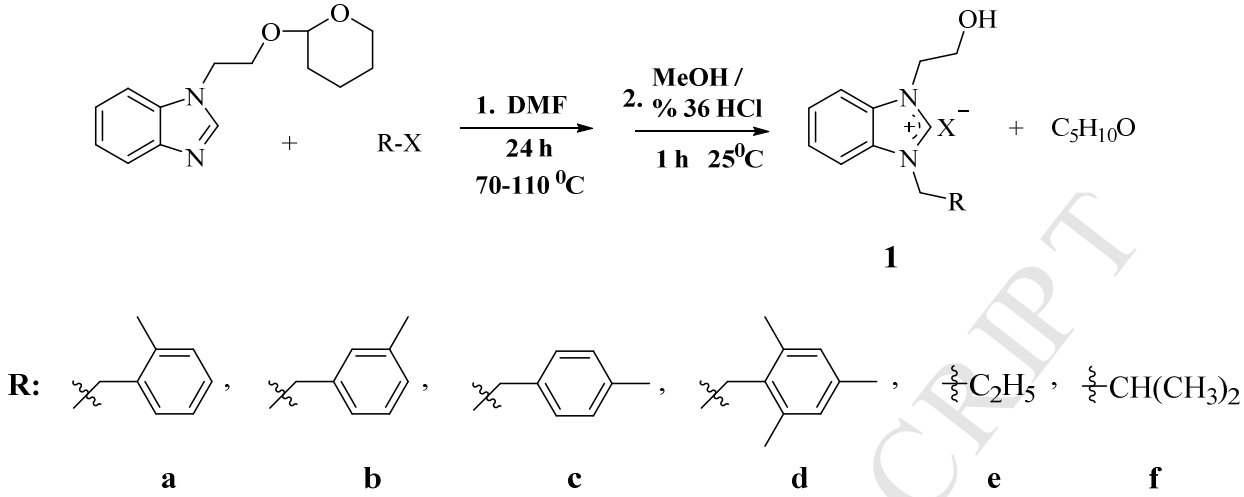

Scheme 1. Synthesis of 2-hydroxyethyl substituted NHC precursor **1a-f**

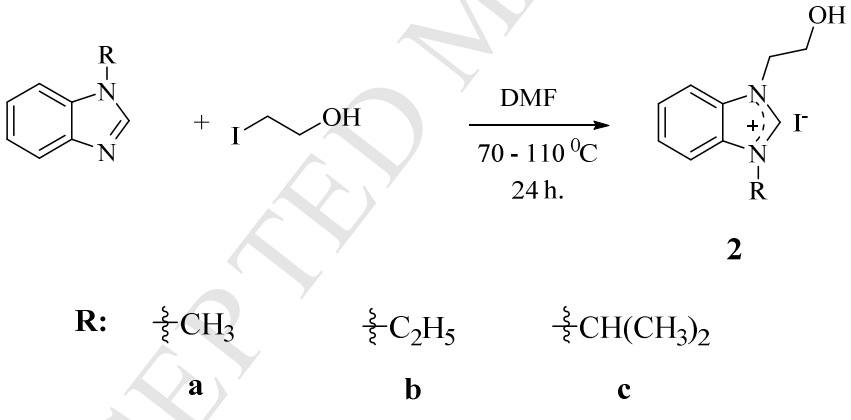

Scheme 2. Synthesis of 2-hydroxyethyl substituted NHC precursor **2a-c**

3.2. Enzyme inhibition studies

Novel synthesized derivatives have recently continued to attract attention, as many enzyme inhibitors. In this study both CA isoforms (hCA I & II) were firstly purified by affinity chromatography sepharose-4B-L-tyrosine-sulfanilamide in a single purification step. The eluates protein from the column were measured spectrophotometrically at 280 nm. CA isoforms activities were measured according to a procedure recorded by Verpoorte et al.. The changes in

the absorbance at 348 nm for 4-nitrophenylacetate to 4-nitrophenolate was fallowed kinetically for 3 min by using a spectrophotometer. CA isoenzymes have attracted this type of interest for the design of inhibitors or activators with pharmaceutical and physiological biomedical applications. In this study, inhibition properties of some novel 2-hydroxyethyl substituted NHC precursors against hCA I and II isoenzymes were determined. For both isoenzymes, esterase activity method was used for determination of IC_{50} values as inhibition parameter. The range of IC_{50} value for hCA I inhibition was determined from 0.1565±0.178 to 0.5127±0.043 μM as shown in Table 2 and Fig. 2a. Compound **2c** showed the lowest IC_{50} value found as 0.1565±0.178 μM, on the other side compound **1b** showed the highest IC_{50} value as 0.5127±0.043 μM, on the other side the range of IC_{50} value for hCA II inhibition was determined from 0.1524±0.013 to 0.5368±0.042 μM. Compound **1d** showed the lowest IC_{50} value as 0.1524±0.013 μM, on the other side compound **1a** showed the highest IC_{50} value as 0.5368±0.042 μM. Cytosolic hCA I and II are expressed in red blood cells and are necessary for maintaining the physiological pH of the blood through production of HCO_3^-. Abnormal levels of CA I in the blood are used as a marker for hemolytic anemia. Behçet *at al.* found that 2-(4-hydroxyphenyl)ethyl and 2-(4-nitrophenyl)ethyl substituted benzimidazolium salts were inhibited the cytosolic isoform hCA I and hCA II, with IC_{50} values in the range from 40.81 to 79.92 nM and from 44.91 to 107.02, respectively [31]. In this study, the **2c** compound contains the iodide anion. Therefore, the solubility of this compound in the water system is higher than **1a-f.** The 2c compound has also more steric bulk due to isopropyl group compared with **2a-2b** (containing methyl and ethyl groups). This steric bulk provides interaction between salt, and active center of the enzymes. Thus, the decrease in the IC_{50} values of the compound **2c** has observed. These results are similar with the inhibition level of our some 2-hydroxyethyl substituted NHC precursors [30].

The XO inhibitory activities of 2-hydroxyethyl substituted NHC precursors are given in Table 2 and Fig. 2b, as half maximal inhibitory micromolar concentration (IC_{50}) values. The experimental results indicated that all 2-hydroxyethyl substituted NHC precursors showed remarkable inhibition activity toward XO as compared with the standard allopurinol. The range of IC_{50} value for XO inhibition was determined from 1.253 ± 0.084 to 5.342 ± 0.168 μM as shown in Table 2

and Fig. 2. Compound **1d** showed the lowest IC_{50} value found as 1.253 ± 0.084 μM, on the other side compound **1f** showed the highest IC_{50} value as 5.342 μM. The IC_{50} for allopurinol was determined as 4.2 μM as a positive control. Compound **1d** which includes trimethyl benzyl substituent has demonstrated high inhibition effect on hCA I, hCA II and XO compared to other complexes due to trimethylbenzyl substituent compound **1d** has steric bulk that has more Van Der Walls interaction between enzyme and compound. In addition, iodide salts (**2b** and **2c**) have demonstrated more inhibition effect on all enzymes compared to chloride salts (**1e** and **1f**) due to iodide salts have a higher solubility than chloride salts. This property of iodide salts might contribute in higher inhibition activity of complexes. In a previous study, the range of IC_{50} value for XO inhibition was determined from 4.608 to 7.084 μM for some pyrrole carboxamide derivatives by Kıbrız et al. [59] Zhang et al. founded the range from 6.7 to 45 μM for 17 compounds of benzonitrile derivatives as IC_{50} value for XO inhibition [62]. In another study, inhibitory effect of natural plant flavonoids on XO enzyme was found that IC_{50} was in between 4.5 and 21.3 μg/mL [63]. Our results showed that 2-hydroxyethyl substituted NHC precursors have potential inhibition activity against hCA I, hCA II and XO. When examined the Table 2 and Fig. 2, there are some compounds exhibited more XO inhibition activity than allopurinol.

Table 2. The IC_{50} value of 2-hydroxyethyl substituted NHC precursors on both human carbonic anhydrase isoenzymes (hCA I and II) and xanthine oxidase enzyme (XO).

Compounds	IC_{50} (μM)					
	hCA I	r^2	**hCA II**	r^2	**XO**	r^2
1a	0.4875 ± 0.039	0.9895	0.5368 ± 0.042	0.9742	2.445 ± 0.140	0.9997
1b	0.5127 ± 0.043	0.9867	0.4898 ± 0.039	0.9986	4.219 ± 0.079	0.9951
1c	0.3957 ± 0.069	0.9897	0.3186 ± 0.079	0.9768	1.914 ± 0.072	0.9800
1d	0.1746 ± 0.096	0.9876	0.1524 ± 0.013	0.9784	1.253 ± 0.084	0.9771
1e	0.3955 ± 0.072	0.9786	0.3257 ± 0.059	0.9879	5.342 ± 0.168	0.9617
1f	0.4236 ± 0.125	0.9985	0.3646 ± 0.086	0.9897	4.992 ± 0.113	0.9915
2a	0.3568 ± 0.079	0.9879	0.3246 ± 0.178	0.9658	2.877 ± 0.042	0.9888

2b	0.2351 ± 0.057	0.9968	0.1937 ± 0.084	0.9764	1.515 ± 0.013	0.9615
2c	0.1565 ± 0.178	0.9875	0.1859 ± 0.197	0.9876	2.318 ± 0.056	0.9798
Allopurinol					4.2 ± 0.035	0.9796

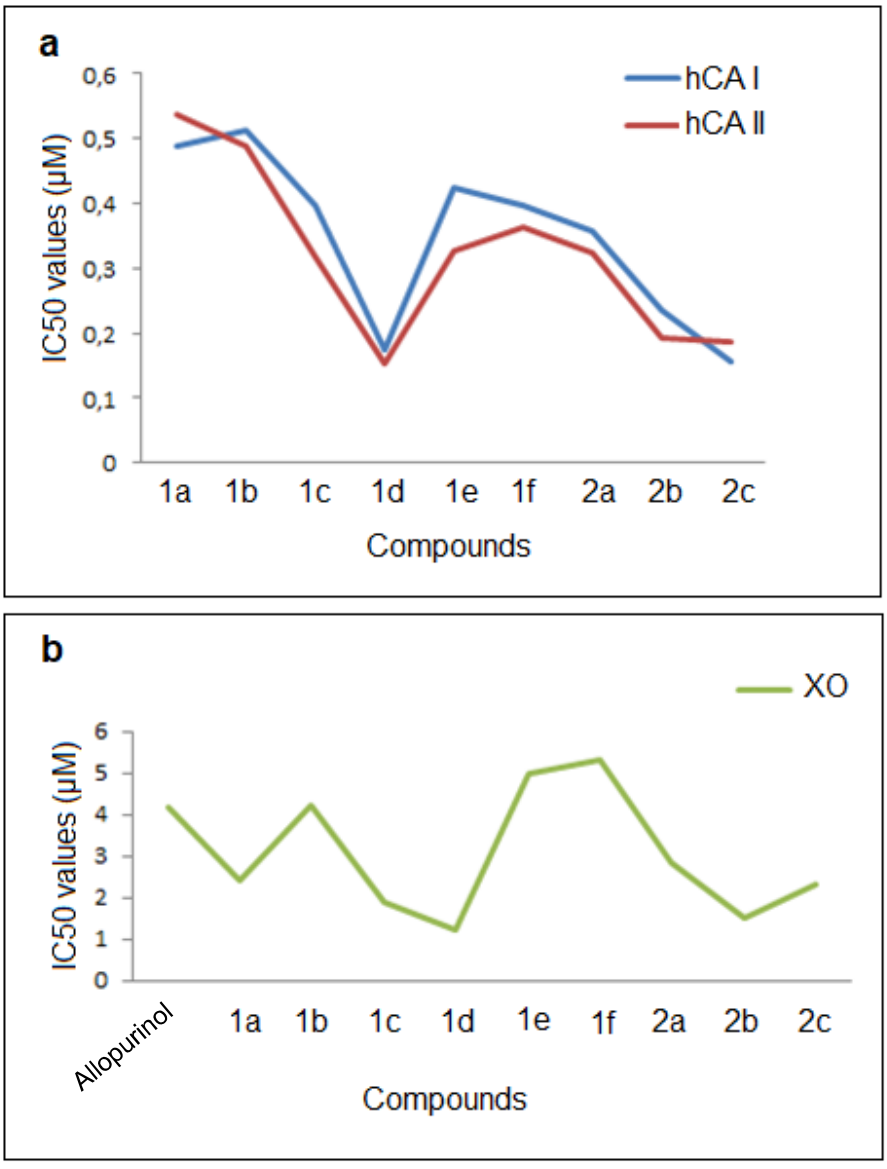

Figure 2. The IC50 values of NHC precursors on a) hCAI and hCAII, b) XO enzymes.

3.3. Structural description of 2a

The molecular structure of **2a** with displacement ellipsoids drawn at 30% probability level is as shown in the Fig. 3. The asymmetric unit contains an iodide anion and a cation features hydroxyethyl and methyl groups substituted to *N*-benzimidazole ring. The single crystal X-ray diffraction studies indicate that the *N*-benzimidazole ring system together with C8 and C9 atoms is essentially coplanar with a mean deviation of 0.013 Å. The hydroxyethyl moiety is tilted towards to the iodide anion with the torsion angle of N2–C9–C10–O1 = -65.4(6)°. Bond parameters such as bond lengths and angles are comparable with our previously published structures of NHC salts consisting iodide ions [30].

Crystal packing of **2a** is consolidated by intramolecular hydrogen bonds and intermolecular weak interactions involving the iodide anion. The I^- ions behave as a H-bond acceptor in the crystal structure, resulting in the formation of two-dimensional supramolecular array (see Table 3 and Fig. 4.). Iodide anions connect the cation molecules with C1–H1A···I1^{i} and C6–H6···I1^{ii} intermolecular interactions along the *a* axis, while connecting the molecules *via* O1–H1···I1 hydrogen bond and C6-H6···I1^{ii} interactions along the *b* axis. In the view of this result, molecules form one-dimensional polymeric infinite zigzag chains along the *a* and *b* axes with the C(7) and C(8) motif, respectively.

Table 3. Intramolecular hydrogen bond and intermolecular weak interactions [Å,°] for **2a.**

Compound	D–H···A	D–H	H···A	D···A	D–H···A
2a	O1–H1···I1	0.90	2.56	3.453(4)	172
	C1–H1A···I1^{i}	0.93	2.88	3.768(5)	160
	C6–H6···I1^{ii}	0.93	3.01	3.926(5)	167

Symmetry codes: (i) 3/2-x, 1/2+y, 1/2-z; (ii) 1/2-x, 1/2+y, 1/2-z

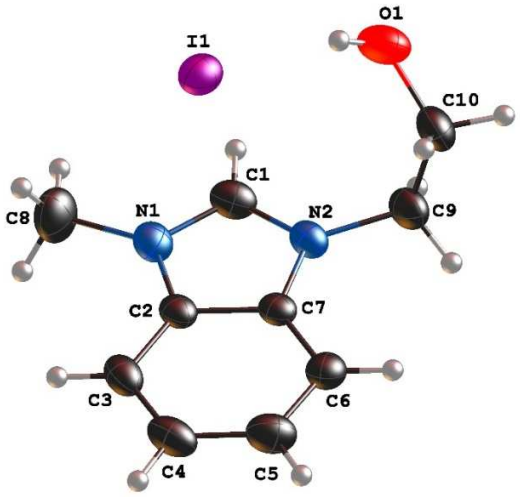

Figure 3. Molecular structure of **2a**, anisotropic displacement parameters depicting 30% probability. Selected bond parameters (Å,°): O1–C10 1.400(6), N1–C1 1.336(5), N1–C2 1.376(5), N1–C8 1.469(5), N2–C1 1.328(6), N2–C7 1.383(5), N2–C9 1.470(5); N1–C1–N2 109.6(4), C1–N1–C8 124.4(4), C1–N2–C9 124.8(4), N2–C9–C10 111.6(3), C9–C10–O1 112.2(4), C8–N1–C2 127.3(4), C9–N2–C7 126.3(4); N1–C1–N2–C9 -177.7(3), N2–C1–N1–C8 179.2(4), C1–N2–C9–C10 86.6(5), N2–C9–C10–O1 -65.4(6), C3–C2–N1–C8 2.0(7), C7–N2–C9–C10 -89.0(5), C6–C7–N2–C9 -4.2(6)

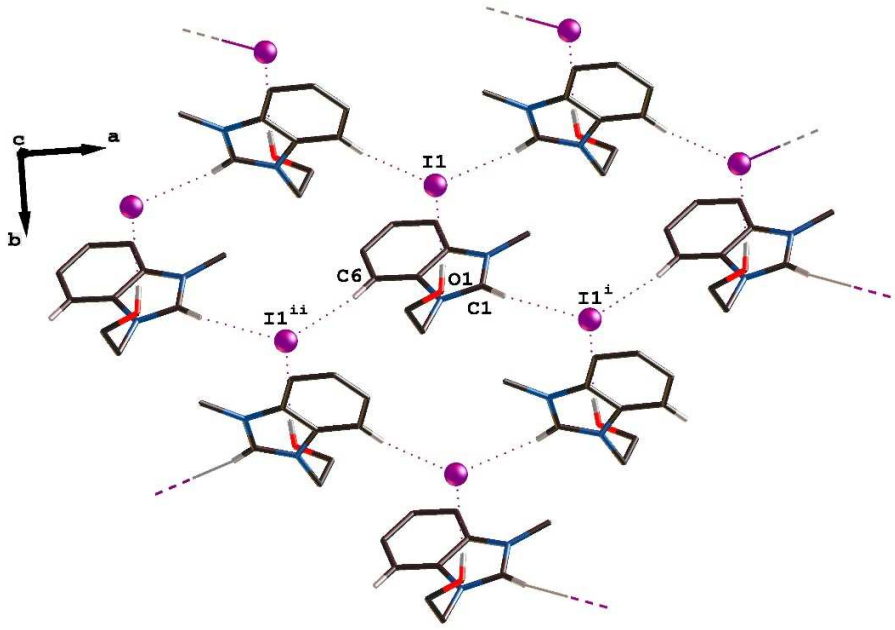

Figure 4. Packing of the cation molecules *via* the intramolecular hydrogen bonds and intermolecular interactions, bridged by the iodide anions, which lead to the infinite chain along the *a* and *b* axes. All

hydrogen atoms except those participating in the hydrogen bonds were omitted for clarity. Cation molecules are shown in stick drawing style.

4. Conclusions

Consequently, we have reported the synthesis of the 2-hydroxyethyl substituted NHC precursors. They have been characterized by ^{1}H NMR, ^{13}C NMR, FTIR spectroscopy and elemental analysis techniques. Molecular and crystal structure of **2a** has been determined by single-crystal X-ray diffraction method. Structural analysis has shown that the iodide ion acts as a H-bond acceptor and plays on important role for the stabilization of crystal structure, considering its contribution to the formation of the 2D supramolecular architecture. All the synthesized 2-hydroxyethyl substituted NHC precursors inhibited metabolic enzymes hCA I, hCA II and XO effectively as compared with the standards.

Conflicts of interests

The authors declare that no conflicts of interests.

Supplementary

Crystallographic data as .cif files for the structures reported in this paper have been deposited at the Cambridge Crystallographic Data Center with CCDC 1878826 for **2a**. Copies of the data can be obtained free of charge at http://www.ccdc.cam.ac.uk/conts/retrieving.html or from the Cambridge Crystallographic Data Center, 12, Union Road, Cambridge CB2 1EZ, UK. Fax: (+44) 1223-336-033, email: deposit@ccdc.cam.ac.uk.

Acknowledgments

This work was financially supported by Inonu University Research Fund (IUBAP FOA-2018-1342). The authors acknowledge Inonu University Scientific and Technology Center for the elemental analyses of the compounds and the authors acknowledge the İnönü University Faculty of Science Department of Chemistry for the characterization of compounds. The authors acknowledge Dokuz Eylül University for the use of the Oxford Rigaku Xcalibur Eos Diffractometer (purchased under University Research Grant No: 2010.KB.FEN.13).

References

1. L. Tschugajeff, M. Skanawy-Grigorjewa, A. Posnjak, About The Hydrazine-Carbylamine Complexes of Platinum, Z. Anorg. Allg. Chem. 148 (1925) 37–42.
2. H.W. Wanzlick, Aspects of nucleophilic carbene chemistry, Angew. Chem. Int. Ed. 1 (1962) 75-80.
3. H.W. Wanzlick, H.J. Schönherr, Direct synthesis of a mercury salt-carbene complex, Angew. Chem. Int. Ed. 7 (1968) 141-142.
4. A.J. Arduengo III, R.L. Harlow, M.Kline, A stable crystalline carbine, J. Am. Chem. Soc., 113 (1) (1991) 361–363.
5. S. Díez-Gonzalez, N. Marion and S. P.Nolan, N-heterocyclic carbenes in late transition metal catalysis, Chem. Rev. 109 (2009) 3612–3676.
6. C. Samojłowicz, M. Bieniek and K. Grela, Ruthenium-based olefin metathesis catalysts bearing N-heterocyclic carbene ligands, Chem. Rev. 109 (2009) 3708–3742.
7. M. Poyatos, J. A. Mata and E. Peris, Complexes with poly (N-heterocyclic carbene) ligands: structural features and catalytic applications, Chem. Rev. 109 (2009) 3677–3707.
8. J. C. Y. Lin, R. T. W. Huang, C. S. Lee, A. Bhattacharyya, W. S. Hwang and I. J. B. Lin, Coinage metal-N-heterocyclic carbene complexes, Chem. Rev. 109 (2009) 3561–3598.
9. P. L. Arnold, I. J. Casely, F-block N-heterocyclic carbene complexes, Chem. Rev. 109 (2009) 3599–3611.
10. S. Bellemin-Laponnaz, S. Dagorne, Group 1 and 2 and early transition metal complexes bearing N-heterocyclic carbene ligands: coordination chemistry, reactivity, and applications, Chem. Rev. 114 (2014) 8747–8774.
11. O. Kühl, The chemistry of functionalised N-heterocyclic carbenes, Chem. Soc. Rev. 36 (2007) 592–607.
12. D. Pugh and A. A. Danopoulos, Metal complexes with 'pincer'-type ligands incorporating N-heterocyclic carbene functionalities, Coord. Chem. Rev. 251 (2007) 610–641.
13. S. T. Liddle, I. S. Edworthy and P. L. Arnold, Anionic tethered N-heterocyclic carbene chemistry, Chem. Soc. Rev. 36 (2007) 1732–1744.
14. K. Riener, S. Haslinger, A. Raba, M. P. Högerl, M. Cokoja, W. A. Herrmann and F. E. Kühn, Chemistry of iron N-heterocyclic carbene complexes: syntheses, structures, reactivities, and catalytic applications, Chem. Rev. 114 (2014) 5215–5272.

15. R. H. Crabtree, NHC ligands versus cyclopentadienyls and phosphines as spectator ligands in organometallic catalysis, J. Organomet. Chem. 690 (2005) 5451–5457.

16. D. J. Nelson and S. P. Nolan, Quantifying and understanding the electronic properties of N-heterocyclic carbenes, Chem. Soc. Rev. 42 (2013) 6723–6753.

17. A. Aktaş, Y. Gök, 4-Vinilbenzil-ornatılmış gümüş (I) N -heterosiklik karben kompleksleri ve rutenyum (II) N -heterosiklik karben kompleksleri: ketonların sentezi ve transfer hidrojenasyonu, Transit. Met. Chem. 39 (2014) 925–931.

18. A. Aktaş, Y. Gök, N-Propylphthalimide-Substituted Silver(I) N-Heterocyclic Carbene Complexes and Ruthenium(II) N-Heterocyclic Carbene Complexes: Synthesis and Transfer Hydrogenation of Ketones, Catal Lett. 145 (2015) 631–639.

19. Y. Sarı, A. Aktaş, D.B. Celepci, Y. Gök, M. Aygün, Synthesis, Characterization and Crystal Structure of New 2-Morpholinoethyl-Substituted Bis-(NHC)Pd(II) Complexes and the Catalytic Activity in the Direct Arylation Reaction, Catal. Lett. 147 (2017) 2340–2351.

20. H. Erdoğan, A. Aktaş, Y. Gök, Y. Sarı, N-Propylphthalimide-substituted bis-(NHC) PdX 2 complexes: synthesis, characterization and catalytic activity in direct arylation reactions, Transit. Met. Chem. 43 (2018) 31–37.

21. A. Aktaş, Y. Gök, H. Erdoğan, Y. Sarı, New 4-vinylbenzyl-substituted bis (NHC)-Pd (II) complexes: Synthesis, characterization and the catalytic activity in the direct arylation reaction, Inor. Chim. Acta. 471 (2018) 735-740.

22. Y.Gök, A. Aktaş, Y. Sarı, H. Erdoğan, 2-methyl-1,4-benzodioxan-substituted bis(NHC)PdX_2 complexes: Synthesis, characterization and the catalytic activity in the direct arylation reaction of some 2-alkyl-heterocyclic compounds, J. Iran Chem. Soc. doi.org/10.1007/s13738-018-1512-y

23. I Yıldırım, A Aktaş, D Barut Celepci, S Kırbağ, T Kutlu, Y Gök, M Aygün, Synthesis, characterization, crystal structure, and antimicrobial studies of 2-morpholinoethyl-substituted benzimidazolium salts and their silver(I)-N-heterocyclic carbene complexes, Res. Chem. Intermed. 43 (2017) 6379–6393.

24. B T. Elie, Y Pechenyy, F Uddin, M. Contel, A heterometallic ruthenium–gold complex displays antiproliferative, antimigratory, and antiangiogenic properties and inhibits metastasis and angiogenesis-associated proteases in renal cancer, Journal of Biological Inorganic Chemistry 23 (2018) 399–411.

25. C. Zhang, M-L. Maddelein, R. W-Y Sun, H. Gornitzka, O. Cuvillier, C. Hemmert, Pharmacomodulation on Gold-NHC complexes for anticancer applications–is lipophilicity the key point?, European Journal of Medicinal Chemistry 157 (2018) 320-332.

26. A Aktaş, Ü Keleştemur, Y Gök, S Balcıoğlu, B Ateş, M Aygün, 2-Morpholinoethyl-substituted N-heterocyclic carbene (NHC) precursors and their silver(I)NHC complexes: synthesis, crystal structure and in vitro anticancer properties, J. Iran Chem. Soc. 15 (2018) 131–139.

27. A. Aktas¸, P. Taslimi, I. Gülcin, Y. Gök, Novel NHC Precursors: Synthesis, Characterization, and Carbonic Anhydrase and Acetylcholinesterase Inhibitory Properties, Arch. Pharm. Chem. Life Sci. 350 (2017) doi.org/10.1002/ardp.201700045.

28. F. Türker, D. Barut Celepci, A. Aktaş, P. Taslimi, Y. Gök, M. Aygün, İ. Gülçin, meta-Cyanobenzyl substituted benzimidazolium salts: Synthesis, characterization, crystal structure and carbonic anhydrase, α-glycosidase, butyrylcholinesterase, and acetylcholinesterase inhibitory properties, Arch. Pharm. Chem. Life Sci. doi.org/10.1002/ardp.201800029.

29. Y. Sarı, A. Aktaş, P. Taslimi, Y.Gök, İ. Gulçin, Novel N-propylphthalimide- and 4-vinylbenzyl-substituted benzimidazole salts: Synthesis, characterization, and determination of their metal chelating effects and inhibition profiles against acetylcholinesterase and carbonic anhydrase enzymes, J. Biochem. Mol. Toxicol. (2017) doi.org/10.1002/jbt.22009.

30. F. Erdemir, D. Barut Celepci, A. Aktaş, P. Taslim, Y. Gök, H. Karabıyık, İ. Gülçin, 2-Hydroxyethyl substituted NHC precursors: Synthesis, characterization, crystal structure and carbonic anhydrase, α-glycosidase, butyrylcholinesterase, and acetylcholinesterase inhibitory properties, Journal of Molecular Structure 1155 (2018) 797-806.

31. A. Behçet, T. Çağlılar, D. Barut Celepci, A. Aktaş, P. Taslim, Y. Gök, M. Aygün, R. Kaya, İ. Gülçin, Synthesis, characterization and crystal structure of 2-(4-hydroxyphenyl)ethyl and 2-(4-nitrophenyl)ethyl Substituted Benzimidazole Bromide Salts: Their inhibitory properties against carbonic anhydrase and acetylcholinesterase, Journal of Molecular Structure 1170 (2018) 160-169.

32. B. Yiğit, M. Yiğit, D. Barut Celepci, Y. Gök, A. Aktaş, M. Aygün, P. Taslimi, İ. Gülçin, Novel Benzylic Substituted Imidazolinium, Tetrahydropyrimidinium and

Tetrahydrodiazepinium Salts: Potent Carbonic Anhydrase and Acetylcholinesterase Inhibitors, Chemistry Select 3 (2018) 7976–7982.

33. U.M. Koçyigit, O.N. Aslan, İ. Gülçin, Y. Temel, M. Ceylan, Synthesis and carbonic anhydrase inhibition of novel 2-(4-(aryl)thiazole-2-yl)-3a,4,7,7a-tetrahydro-1h-4,7-methanoisoindole-1,3(2h)-dione derivatives. Arch. Pharm. Chem. Life Sci. 349(12) (2016) 955-963.

34. K. Kücükoğlu, F. Oral, T. Aydın, C. Yamalı, O. Algül, H. Sakagami, H.İ. Gül, Synthesis, cytotoxicity and carbonic anhydrase inhibitory activities of new pyrazolines, Journal of Enzyme Inhibition and Medicinal Chemistry, 31(S4) (2016) 20-24.

35. H.İ. Gül, E. Mete, P. Taslimi, İ. Gülçin, C.T. Supuran, Synthesis, carbonic anhydrase I and II inhibition studies of the 1, 3, 5-trisubstituted-pyrazolines. Journal of Enzyme Inhibition And Medicinal Chemistry, 32(1) (2017) 189-192.

36. H. Göçer, F. Topal, M. Topal, M. Küçük, D. Teke, İ. Gülçin, C.T. Supuran, Acetylcholinesterase and carbonic anhydrase isoenzymes I and II inhibition profiles of taxifolin. Journal of Enzyme Inhibition and Medicinal Chemistry, 31(3) (2016) 441-447.

37. A. Scozzafava, A. Mastrolorenzo, C.T. Supuran, Expert Opin Ther Pat 14 (2004) 667–702.

38. P.J. Wistrand, W.R. Chegwidden, N.D. Carter, Y.H. Edwards, The carbonic anhydrases: New horizons. Basel: Birkhaüser Verlag; (2000) 597–609.

39. S. Parkkila, A-K. Parkkila, J. Kivela, C.T. Supuran, A. Scozzafava, J. Conway, Carbonic anhydrase: Its inhibitors and activators, Boca Raton, FL: CRC Press (2004) 283–301.

40. T.H. Maren W.R. Chegwidden, N.D. Carter, Y.H. Edwards, The carbonic anhydrases: New horizons. Basel: Birkhaüser Verlag; (2000) 425–436.

41. A. Akıncıoğlu, M. Topal, İ. Gülçin, S. Göksu, Novel sulphamides and sulphonamides incorporating the tetralin scaffold as carbonic anhydrase and acetylcholine esterase inhibitors. Archiv der Pharmazie, 347(1) (2014) 68-76.

42. A. Bhatt, B.P. Mahon, V.W.D. Cruzeiro, B. Cornelio, M. Laronze Cochard, M. Ceruso, A. Roitberg, Structure–activity relationships of benzenesulfonamide based inhibitors towards carbonic anhydrase isoform specificity. Chembiochem, 18(2) (2017) 213-222.

43. H. Göcer, A. Akıncıoğlu, S. Göksu, İ. Gülçin, Carbonic anhydrase inhibitory properties of phenolic sulfonamides derived from dopamine related compounds, Arab. J. Chem. 10 (2017) 398–402.

44. N. Öztaşkın, Y. Çetinkaya, P. Taslimi, S. Göksu, İ. Gülçin, Antioxidant and acetylcholinesterase inhibition properties of novel bromophenol derivatives, Bioorg. Chem. 60 (2015) 49–57.

45. M. Gliozzi, N. Malara, S. Muscoli, V. Mollace, The treatment of hyperuricemia, Int. J. Cardiol, 213 (2016) 23-27.

46. M. Boban, G. Kocic, S. Radenkovic, R. Pavlovic, T. Cvetkovic, M. Deljanin-Ilic, S. Ilic, M. B. Bobana, B. Djindjic, D. Stojanovic, D. Sokolovic, T. Jevtovic-Stoimenov, Circulating purine compounds, uric acid, and xanthine oxidase/dehydrogenase relationship in essential hypertension and end stage renal disease. Renal Failure 36 (2014) 613−618.

47. E. Borges, E. Fernandes, F. Roleira, Progress towards the discovery of xanthine oxidase inhibitors, Curr. Med. Chem. 9 (2002) 195-217.

48. C. Chen, J.-M. Lü, Q. Yao, Hyperuricemia-related diseases and xanthine oxidoreductase (XOR) inhibitors: an overview, Med Sci Monit, 22 (2016) 2501-2512.

49. J.-M. Lü, Q. Yao, C. Chen, 3, 4-Dihydroxy-5-nitrobenzaldehyde (DHNB) is a potent inhibitor of xanthine oxidase: a potential therapeutic agent for treatment of hyperuricemia and gout, Biochem Pharmacol, 86 (2013) 1328-1337.

50. J. Evenäs, F. Edfeldt, M. Lepistö, N. Svitacheva, A. Synnergren, B. Lundquist, M. Gränse, A. Rönnholm, M. Varga, J. Wright et al. HTS followed by NMR based counterscreening. Discovery and optimization of pyrimidones as reversible and competitive inhibitors of xanthine oxidase, Biorg. Med. Chem. Lett. 24 (2014) 1315-1321.

51. D. Yasuda, K. Takahashi, T. Kakinoki, Y. Tanaka, T. Ohe, S. Nakamura, T. Mashino, Synthesis, radical scavenging activity and structure–activity relationship of uric acid analogs, MedChemComm. 4 (2013) 527-529.

52. P. Pacher, A. Nivorozhkin, C. Szabo, Therapeutic effects of xanthine oxidase inhibitors: renaissance half a century after the discovery of allopurinol, Pharmacol. Rev. 58 (2006) 87-114.

53. A. Aktaş, D. Barut Celepci, Y. Gök, M. Aygün, 2-Hydroxyethyl-Substituted Pd-PEPPSI Complexes: Synthesis, Characterization and the Catalytic Activity in the Suzuki-Miyaura Reaction for Aryl Chlorides in Aqueous Media, ChemistrySelect 3 (2018) 9974 –9980.

54. A. Aktaş, D. Barut Celepci, Y. Gök, M. Aygün, 2-Hydroxyethyl-Substituted (NHC)Pd(II)PPh_3 Complexes: Synthesis, Characterization, Crystal Structure and Its

Application on Sonogashira Cross-Coupling Reactions in Aqueous Media, ChemistrySelect 3 (2018) 10932– 10937.

55. A. Aktaş, F. Erdemir, D. Barut Celepci, Y. Gök, M. Aygün, Mixed phosphine/N‐heterocyclic carbene–palladium complexes: synthesis, characterization, crystal structure and application in the Sonogashira reaction in aqueous media, Transit. Met. Chem. (2018) doi.org/10.1007/s11243-018-0286-5

56. CrysAlis^{Pro} Software System, Version 1.171.38.43 (Rigaku Corporation, Oxford, UK. (2015)

57. G.M. Sheldrick, SHELXT - Integrated space-group and crystal-structure determination, Acta Crystallog. Sect. A 71 (2015) 3-8.

58. O.V. Dolomanov, L. J. Bourhis, R. J. Gildea, J. A. K. Howard, H. Puschmann, OLEX2: a complete structure solution, refinement and analysis program. J. Appl. Cryst. 42 (2009) 339-341.

59. G.M. Sheldrick, Crystal structure refinement with SHELXL. Acta Crystallog. Sect. C 71 (2015) 3-8.

60. H. Göçer, A. Akıncıoğlu, S. Göksu, İ. Gülçin, Carbonic anhydrase inhibitory properties of phenolic sulfonamides derived from dopamine related compounds. Arabian Journal of Chemistry 10 (2017) 398–402.

61. İ.E. Kıbrız, M. Saçmacı, İ. Yıldırım, S. Abbas Ali Noma, T. Taşkın Tok, B. Ateş, Xanthine oxidase inhibitoryactivity of new pyrrole carboxamide derivatives:In vitroandin silicostudies. ArchP harm Chem LifeSci. (2018) 351-360.

62. T. Zhang, S. Li, Z. Yi, Q. Wu, F. Meng, Design, synthesis and biological evaluation of 5-(4-(pyridin-4-yl)-1H-1,2,3-triazol-1-yl)benzonitrile derivatives as xanthine oxidase inhibitors. Chem Biol Drug Des; 91 (2017) 526–533.

63. H.S. Nile, S.Y. Keum, S.A. Nile, Antioxidant, anti-inflammatory, and enzyme inhibitory activity of natural plant flavonoids and their synthesized derivatives. J BiochemMol Toxicol. 32 (2017) e22002.

Highlight

1. The 2-hydroxyethyl substituted NHC precursors have been prepared.
2. The 2-hydroxyethyl substituted NHC precursors have been characterized by using spectroscopy and elemental analysis techniques.
3. The 2-hydroxyethyl substituted NHC precursors were investigated against the cytosolic carbonic anhydrase I and II isoenzymes (hCA I and hCA II), and xanthine oxidase (XO).
4. The structure of a new 2-hydroxyethyl substituted NHC precursor was established by using single-crystal X-ray diffraction method.